Stem Cell Reports
Article

ISSCR

OPEN ACCESS

Vitamin C-Induced Epigenetic Modifications in Donor NSCs Establish Midbrain Marker Expressions Critical for Cell-Based Therapy in Parkinson's Disease

Noviana Wulansari,[1,2,3,4] Eun-Hee Kim,[1,2,3,4] Yanuar Alan Sulistio,[1,2,3] Yong-Hee Rhee,[1,2,3] Jae-Jin Song,[1,2,3] and Sang-Hun Lee[1,2,3,*]

[1]Department of Biochemistry and Molecular Biology, College of Medicine, Hanyang University, 17 Haengdang-dong, Sungdong-gu, Seoul 133-791, Korea
[2]Hanyang Biomedical Research Institute, Hanyang University, Seoul, Korea
[3]Graduate School of Biomedical Science and Engineering, Hanyang University, Seoul, Korea
[4]Co-first author
*Correspondence: leesh@hanyang.ac.kr
http://dx.doi.org/10.1016/j.stemcr.2017.08.017

SUMMARY

Cultured neural stem/precursor cells (NSCs) are regarded as a potential systematic cell source to treat Parkinson's disease (PD). However, the therapeutic potential of these cultured NSCs is lost during culturing. Here, we show that treatment of vitamin C (VC) enhances generation of authentic midbrain-type dopamine (mDA) neurons with improved survival and functions from ventral midbrain (VM)-derived NSCs. VC acted by upregulating a series of mDA neuron-specific developmental and phenotype genes via removal of DNA methylation and repressive histone code (H3K9m3, H3K27m3) at associated gene promoter regions. Notably, the epigenetic changes induced by transient VC treatment were sustained long after VC withdrawal. Accordingly, transplantation of VC-treated NSCs resulted in improved behavioral restoration, along with enriched DA neuron engraftment, which faithfully expressed midbrain-specific markers in PD model rats. These results indicate that VC treatment to donor NSCs could be a simple, efficient, and safe therapeutic strategy for PD in the future.

INTRODUCTION

Parkinson's disease (PD) is a common neurodegenerative disorder characterized by progressive degeneration of dopamine (DA) neurons in the midbrain substantia nigra (Savitt et al., 2006). Fetal midbrain transplantation has been clinically performed in PD patients, and has resulted in therapeutic effects (Piccini et al., 1999). However, limited donor tissue, inconsistent therapeutic outcomes, and dyskinesia side effects (Dunnett et al., 2001; Freed et al., 2001) prevented this approach from becoming a generalized therapeutic tool. These problems could be solved by culturing neural stem/precursor cells (NSCs) derived from dopaminergic ventral midbrain (VM) tissues, in which the quality and quantity of transplanted DA neurons could be systematically manipulated.

Midbrain-type DA (mDA) neurons are generated efficiently *in vitro* in NSCs cultured from the VM during early embryonic days, such as rat embryonic days 11–12 (E11–E12) (Lee et al., 2003; Studer et al., 1998). DA neurogenic potential, however, declines severely during *in vitro* NSCs expansion (Lee et al., 2003; Studer et al., 1998; Yan et al., 2001). In addition, expression of midbrain-specific markers FOXA2, LMX1A/B, and NURR1, critical for mDA neuron functions, survival, and phenotype maintenance (Decressac et al., 2013; Oh et al., 2015), is also lost during culturing VM-NSCs (Oh et al., 2015; Rhee et al., 2016). Additionally, NSCs expanded *in vitro* exhibit increased apoptotic cell death during or after differentiation, resulting in poor graft formation after transplantation (Anderson et al., 2007; Ko et al., 2009; Rhee et al., 2011, 2016). Methods to halt these culture-dependent changes need to be developed to generate a systematic source of therapeutically competent donor cells for cell therapeutic approaches for PD.

Vitamin C (L-ascorbic acid; VC) is a crucial microconstituent in most tissues (Monfort and Wutz, 2013). VC concentration is highest in the brain, and even higher during embryonic development (Kratzing et al., 1985), suggesting specific VC roles during brain development. We and other groups have shown that VC promotes DA neuron differentiation by facilitating DA phenotype expression (He et al., 2015; Lee et al., 2003; Yan et al., 2001), suggesting that VC treatment can be utilized in cell-based PD therapy. However, systematic analyses on the practical utility of using VC in PD cell therapy have not been attempted.

In this study, we show that VC treatment during VM-NSC expansion substantially rescues all the culture-dependent changes associated with the therapeutic capacity of donor NSCs in PD cell therapy. The effects of VC were achieved by inducing long-lasting epigenetic modifications to a set of mDA neuron developmental and phenotype genes.

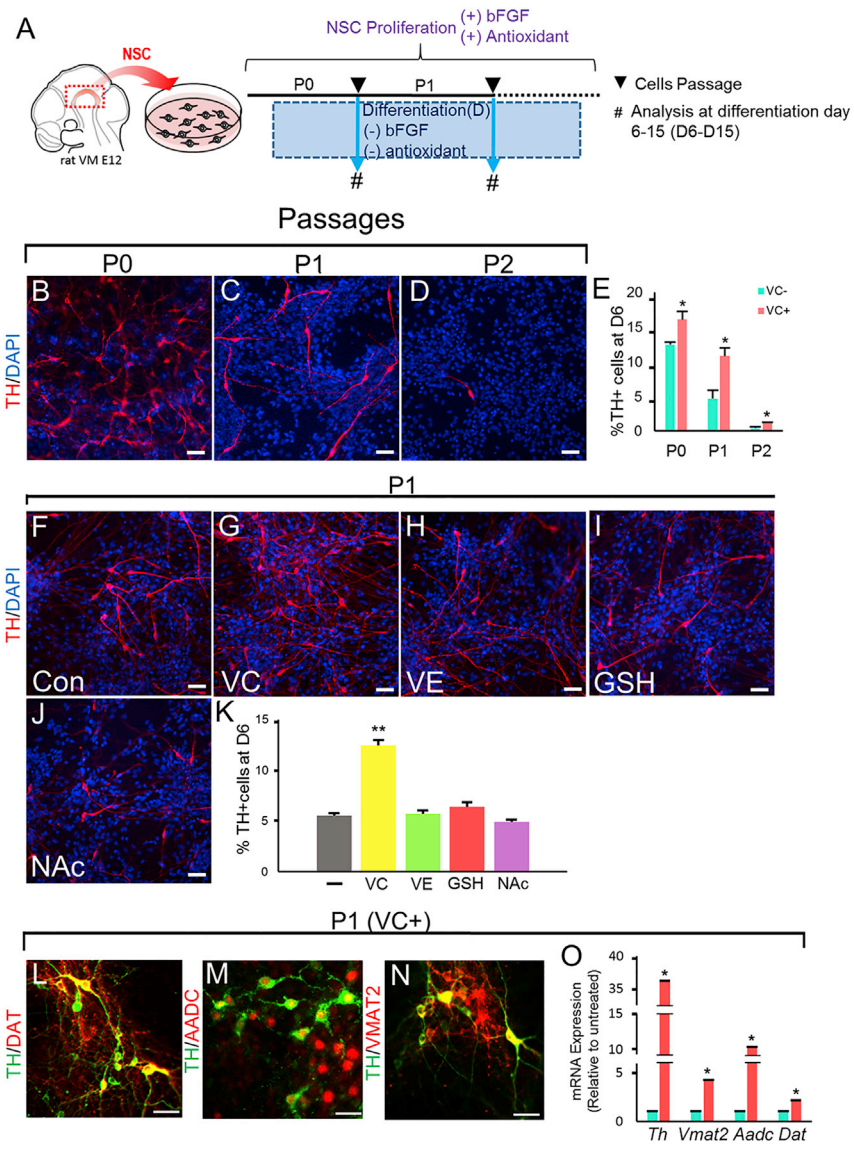

Figure 1. Vitamin C Treatment during VM-NSC Proliferation Rescued the Loss of DA Neurogenic Potential during *In Vitro* Expansion

(A) Schematic of the experimental design.

(B–D) Decline of DA neurogenic potential during *in vitro* cell expansion with serial passages in control VM-NSC cultures (without anti-oxidant treatment). Shown are representative images for TH^+ DA neurons at differentiation day 6 (d6) in unpassaged cultures (P0, B), and cultures passaged one (P1, C) and two (P2, D) times.

(E) DA neuronal yields (percent TH^+ cells of total $DAPI^+$ cells) are depicted as blue bars (control) and red bars (VM-NSCs expanded with VC [200 μM] during P0–P2).

(F–K) DA neuronal yields of the NSC cultures expanded for 8 days (up to P1) in the presence or absence of various anti-oxidant treatments. Shown are representative images of TH^+ DA neurons (F–J) and a quantitative graph (K). Values represent the mean ± SEM; n = 3 independent experiments at $^*p < 0.05$ or $^{**}p < 0.01$, Student's t test (E) and one-way ANOVA with Tukey's post hoc analysis (K). Scale bar, 50 μm.

(L–O) VM-NSCs expanded with VC treatment yield TH^+ DA neurons equipped with other DA neuron phenotypic markers. P1 cultures expanded with VC were differentiated in the absence of VC for 12 days and subjected to co-immunostaining with DAT (L), AADC (M), and VMAT2 (N). Along with an increase in *Th* mRNA expression, expression of other DA phenotype markers at d12 increased upon VC treatment during the expansion period (O). $^*p < 0.01$, n = 3 independent experiments, Student's t test. Scale bar, 50 μm.

RESULTS

VC Rescued Loss of DA Neurogenic Potential during *In Vitro* Expansion of VM-NSCs

NSCs were isolated from naive rat embryo dopaminergic VMs at E12, and expanded in the presence of the mitogen basic fibroblast growth factor (bFGF) *in vitro*. Proliferating VM-NSCs were passaged every 4 days, and cells at each passage were induced to differentiate by withdrawing the mitogen (Figure 1A). The VM-NSCs expanded for a short period (4 days, unpassaged [P0]) and efficiently differentiated into DA neurons expressing tyrosine hydroxylase (TH), the key enzyme for DA biosynthesis; however, DA neuron differentiation was steeply decreased by longer expansion with increased cell passages (Figures 1B–1E). Altered cellular characteristics, including decreased differentiation potential during *in vitro* expansion, are commonly observed in stem/precursor cell cultures derived from mammalian tissues, regardless of tissue origin. This may be regarded as a phenomenon associated with cellular aging, given that similar changes in stem cell properties are manifest during *in vivo* aging (Chang et al., 2004a; Kim et al., 2012). As reactive oxygen species (ROS) are a major cause of cellular aging and senescence, we tested whether elimination of ROS by anti-oxidant treatment in VM-NSC cultures could rescue the culture-dependent loss of DA neurogenic potential. To this end, the anti-oxidants VC, vitamin E, reduced glutathione, or N-acetylcysteine were used as supplements during *in vitro* VM-NSC expansion, and subsequent culture differentiation was induced

without the anti-oxidants (Figure 1A). ROS scavenging effects of all the anti-oxidants tested were confirmed by 2′,7′-dichlorofluorescin staining (Figure S1A). However, among the tested anti-oxidants, only treatment with VC resulted in the prevention of DA neuron loss in passaged cultures (Figures 1F–1K), indicating that VC-specific actions, rather than general anti-oxidant effects, were responsible for the observed VC effect. VC treatment during NSC expansion was dramatic in cultures up to passage 1 (P1), which yielded P1 cultures, in which the TH^+ cell yields (10.85% ± 1.2% of total $DAPI^+$ cells) were as great as those achieved in untreated cultures at P0 (12.5% ± 0.35%) (Figure 1E). Virtually all the TH^+ cells differentiated from VC-treated VM-NSCs at P1 expressed the other DA phenotypes (VMAT2, AADC, and DAT) (Figures 1L–1N) along with increases of their gene expression (Figure 1O), suggesting that VC treatment not only induced TH expression but exerted an effect on authentic DA neuron differentiation.

The dramatic effect of VC treatment was not sustained in cultures that had undergone one additional passage (at P2), in which TH^+ DA neuronal yields from VC-treated NSCs were also sharply reduced to 1.22% ± 0.1%; this was, however, still significantly greater than the VC-untreated control (0.44% ± 0.22%; $p < 0.05$, $n = 3$ independent experiments) (Figure 1E). Based on these findings, the following experiments were carried out to evaluate the effect of VC using P1 cultures, unless otherwise noted.

Midbrain-Specific Marker Expression, Presynaptic Function, and Toxic Resistance of mDA Neurons Differentiated from VC-Treated VM-NSCs

The effect of VC on DA neuron differentiation has been reported in previous studies (He et al., 2015; Lee et al., 2003; Yan et al., 2001). However, in addition to DA neuron yield, successful cell therapeutic outcome relies on the expression of midbrain phenotypes, neuronal maturation, presynaptic functions, and cell survival of the differentiated DA neurons. To investigate VC effects on those aspects, we applied VC during VM-NSC proliferation followed by VC withdrawal during differentiation. The rationale for the VC withdrawal during differentiation is to closely mimic the cell transplantation condition, whereby VC addition is limited to the donor cell preparation period (before cell transplantation), since the proliferating NSC stage is regarded as the most appropriate stage for cell transplantation, given that extensive cell death is associated with transplanting differentiating/differentiated neurons (Timmer et al., 2006).

mDA neurons are characterized by the continued expression of midbrain-specific developmental factors, such as FOXA2, LMX1A, and NURR1, after termination of development in the adult midbrain. Midbrain factor expression in mDA neurons is critical for their survival and function (Decressac et al., 2013; Oh et al., 2015), but disappears in aged or PD midbrains (Oh et al., 2015). A similar loss of midbrain marker expression is also seen in mDA neurons maintained in culture for long periods of time or after transplantation (Rhee et al., 2016), indicating that it is the prime problem to be solved to permit successful PD cell-based therapy (Kriks et al., 2011). Untreated control cultures at P1 yielded TH^+ DA neurons, only portions of which expressed the midbrain markers NURR1 (62%), FOXA2 (73%), and LMX1A (63%) at differentiation day 6 (d6) (Figures 2A–2C). Interestingly, in addition to enhanced DA neuronal yields, almost all TH^+ DA neurons differentiated from VC-treated NSCs expressed midbrain markers (93% [NURR1], 98% [FOXA2], and 91% [LMX1A]).

In morphometric assessments, total fiber lengths per TH^+ DA neuron were significantly greater in cultures differentiated from VM-NSCs expanded with VC supplementation, compared with untreated control cultures (164 μm versus 134 μm, Figure 2D). The synaptic vesicle-specific markers $synapsin^+$ puncta were more abundantly localized in TH^+ DA neuron neurites differentiated from VC-treated NSCs (Figure 2E). We further observed that presynaptic DA release (Figure 2F) was greater in cultures differentiated from VC-treated NSCs. Taken together, these findings indicate that maturity of DA neurons was morphologically, synaptically, and functionally enhanced by VC pretreatment.

A portion of cells undergo cell death during differentiation. Increased cell death during NSC differentiation is another characteristic of cultured NSCs that have undergone longer periods of cell expansion (data not shown and Rhee et al., 2016). Cell death during/after differentiation was greatly reduced in cultures expanded with VC supplementation, as estimated by ethidium homodimer 1 (EthD-1) positivity at d8 (Figure 2G). In addition, γH2AX foci, a DNA damage indicator observed during PD progression, were greatly reduced in VC pretreated differentiated cultures (Figure 2H). Remarkably lower proportions of DA neurons died after exposure to toxic stimuli induced by H_2O_2 or 6-hydroxydopamine (6-OHDA) in cultures differentiated from NSCs pretreated with VC (Figures 2I and 2J). In addition, TH^+ cells that survived toxin treatment in VC pretreated cultures displayed a healthy neuronal shape with extensive neurite outgrowth, while most of the surviving TH^+ cells in the control cultures had blunted or fragmented neurites (insets of Figures 2I and 2J), a neuronal aging and degenerative phenotype (Hof and Morrison, 2004). We emphasize again that all the effects observed in the differentiated cultures were not directly mediated by VC, as the differentiated cells were cultured in the absence of VC.

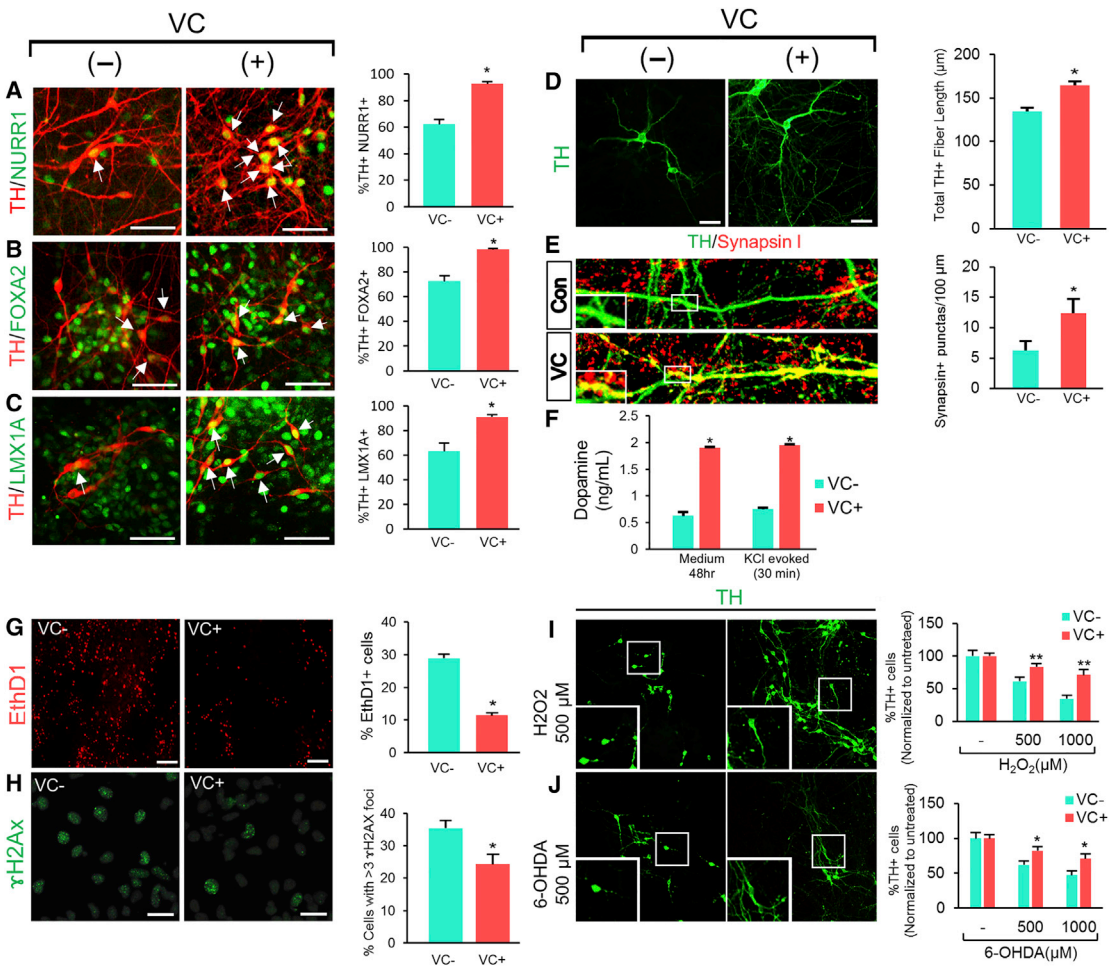

Figure 2. VM-NSCs Expanded with VC Yield DA Neurons with Enhanced Midbrain-Specific Marker Expression, Presynaptic Neuronal Maturation, Cell Survival, and Resistance against Toxic Insults

VM-NSCs were *in vitro* expanded with or without (control) VC up to P1, and then differentiated in the absence of VC for 6–15 days.

(A–C) Co-expression of midbrain-specific markers in differentiated DA neurons. Graphs on the right depict the percentage of TH^+ cells co-expressing the midbrain-specific markers NURR1 (A), FOXA2 (B), and LMX1A (C) out of the total number of TH^+ cells at d6. *$p < 0.001$, n = 30 microscopic fields, Student's t test. White arrows indicate TH^+ DA neurons co-expressing the midbrain markers.

(D–F) Morphological, synaptic, and functional maturity of DA neurons estimated by TH^+ fiber length per DA neuron at d15, n = 60 cells (D), number of $synapsin^+$ puncta along the TH^+ neurites (100 μm; n = 20 neurites) (E), and presynaptic DA release, n = 3 independent experiments (F). Medium (48 hr), DA levels in the media conditioned in the differentiated cultures for 48 hr (d13–15); KCl evoked (30 min), DA levels evoked by KCl-mediated depolarization for 30 min. n = 3 independent experiments. *$p < 0.001$, Student's t test.

(G–J) Effect of VC pretreatment during VM-NSC expansion on differentiated cell survival/death and resistance against toxins. VM-NSCs expanded with or without VC were differentiated for 8 days without VC. General cell death (G) and DNA damage (H) were estimated by the percentage of cells positive for $EthD1^+$ and the percentage of cells with >3 γH2AX foci at d8, respectively. The differentiated cultures at d8 were exposed to H_2O_2 or 6-OHDA (500 μM and 1,000 μM) for 8 hr and viable TH^+ DA neurons were counted on the following day (I and J). *$p < 0.05$ or **$p < 0.01$, n = 3 independent experiments, Student's t test.

Scale bars, 50 μm.

VC-Mediated Epigenetic Control within a Range of mDA Neuron Developmental and Phenotype Genes

In view of VC's anti-oxidant action, mDA neuron differentiation enhanced by VC treatment could be attained by a selective mechanism, in which VC enhanced cell survival and proliferation selectively in DA neuronal lineage cells. However, NSC cultures derived from early rat embryonic brains are highly and sufficiently proliferative and viable in the presence of the mitogen bFGF. Thus, none of the anti-oxidant treatments tested, including VC, significantly altered VM-NSC survival and proliferation up to P1 (the stage during which all analyses in this study were

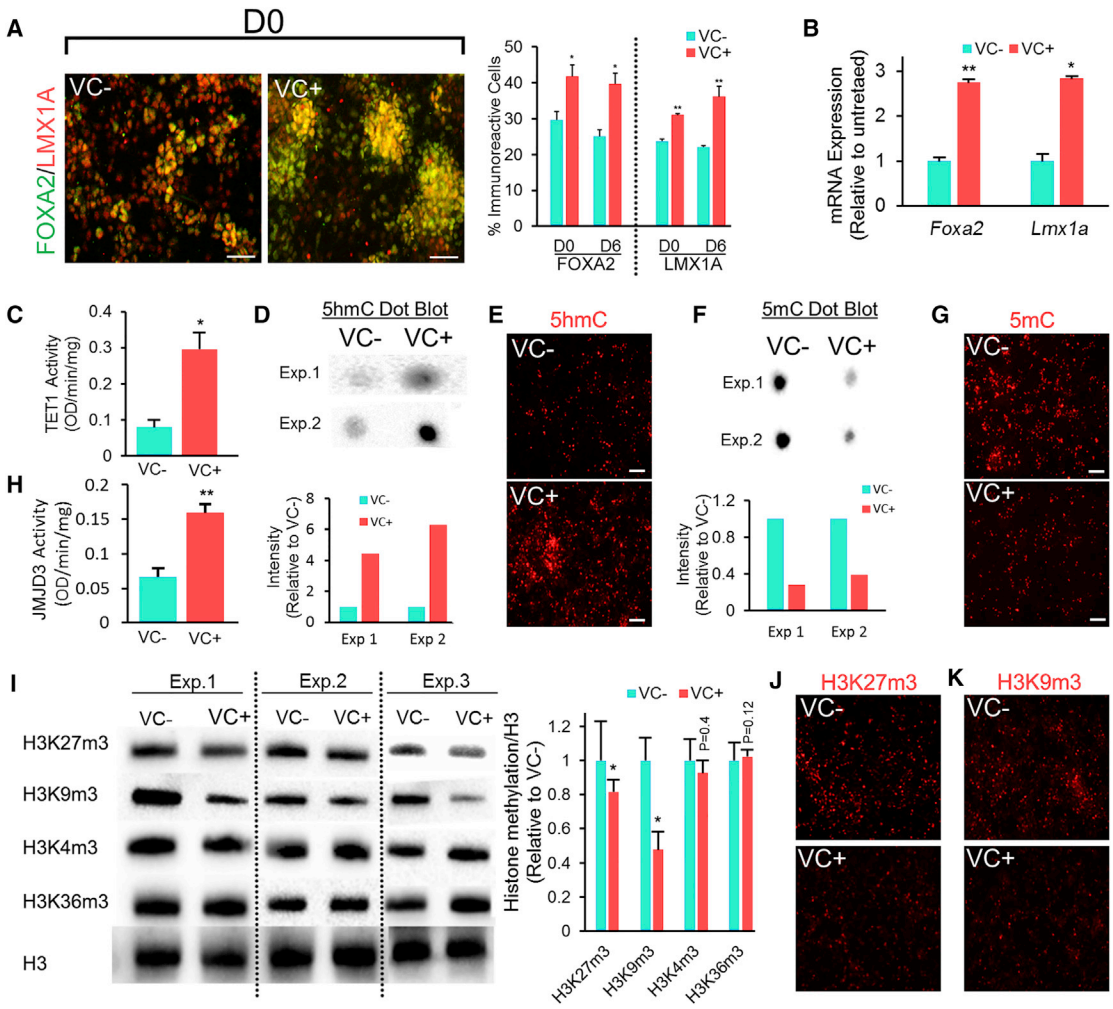

Figure 3. VC Treatment Promoted Expression of FOXA2 and LMX1A in VM-NSCs along with TET1- and Jmjd-Mediated Changes in Global 5hmC/5mC and H3K27m3/H3K9m3 Levels

(A and B) FOXA2 and LMX1A expression in undifferentiated and differentiated VM-NSC cultures estimated by the percentage of immunoreactive cells among total DAPI$^+$ cells at d0 and d6 (A) and real-time PCR at d0 (B).

(C) TET enzyme activity in the nuclear fraction at d0.

(D–G) Global 5hmC (D and E) and 5mC (F and G) levels estimated by DNA dot blot (D and F) and immunocytochemical (E and G) analyses at d0.

(H) JMJD3 enzyme activity.

(I–K) VC effects on global H3K27m3 and H3K9m3 levels estimated by western-blot (I) and immunocytochemical (J and K) analyses at d0. Intensities of the bands in (I) were quantified using ImageJ software, and the values normalized to histone 3 (H3) are depicted in the graph on the right.

Values represent the mean ± SEM; n = 3 independent experiments at *p < 0.05 or **p < 0.01, Student's t test. Scale bars, 50 μm.

done) (Figures S1B and S1C), ruling out the possibility of a selective mechanism in VC-mediated DA neuron differentiation.

Without expression changes of general NSC-specific (Nestin, SOX2) and anterior brain region-specific (OTX2) markers (Figures S2A–S2C), VC treatment during VM-NSC expansion enhanced the percentage of cells expressing the VM-specific NSC markers FOXA2 and LMX1A at d0 (before differentiation induction) (Figure 3A). FOXA2 and LMX1A are expressed in dopaminergic NSCs from early developing VMs and act as the master regulators for mDA neuron development by inducing expression of a battery of later developmental genes, such as NURR1, PITX3, and Neurogenin2 (Ngn2) (Chung et al., 2009; Nakatani et al., 2010; Yi et al., 2014). In addition, as mentioned earlier, expression of FOXA2 and LMX1A that continued in adult

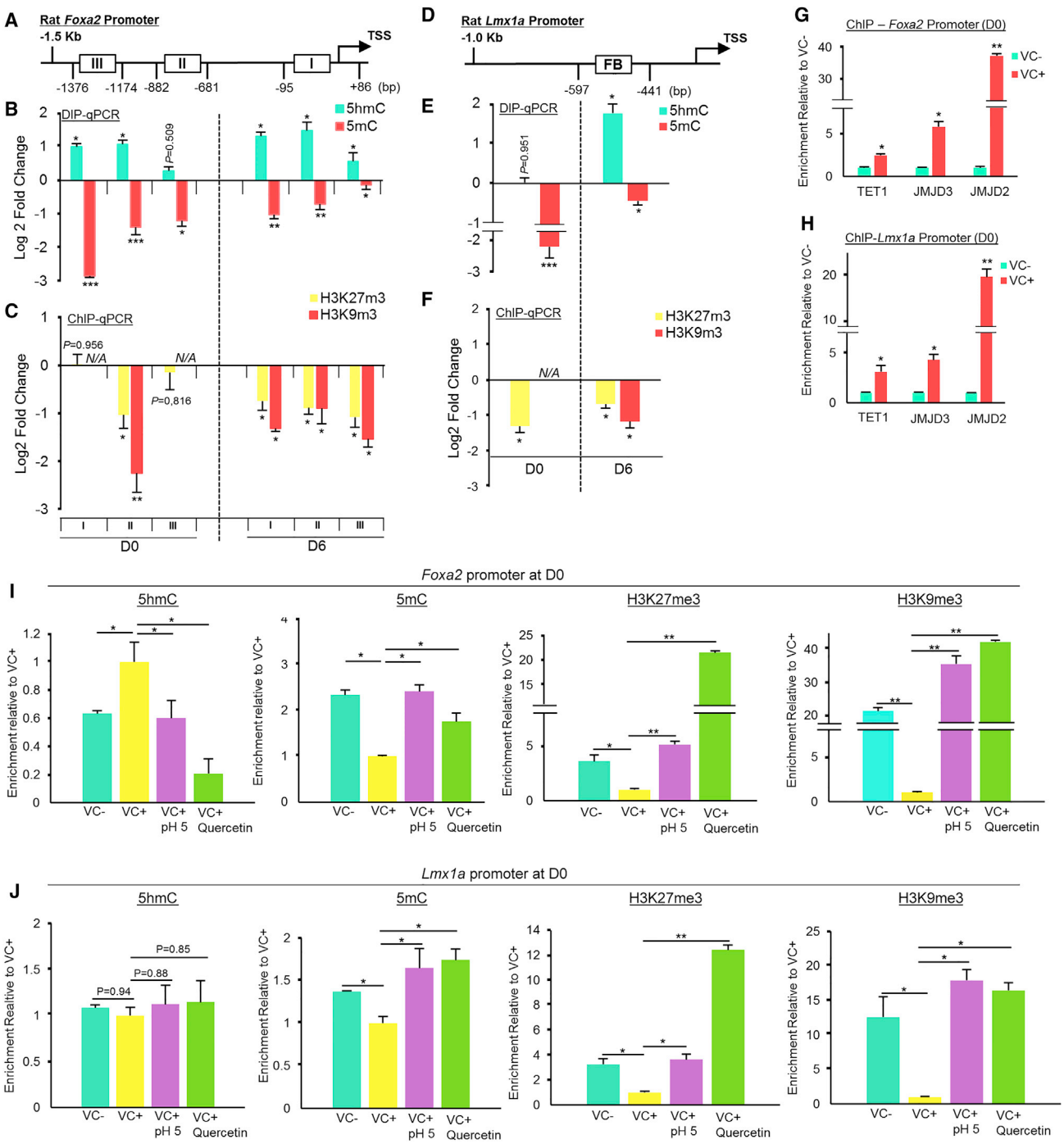

Figure 4. VC-Induced Epigenetic Changes on *Foxa2* and *Lmx1a* Promoters

(A and D) Schematics for the rat *Foxa2* (A) and *Lmx1a* (D) promoters with CpG-enriched regions (indicated by box) targeted for the DIP- and ChIP-PCR analyses. In the *Lmx1a* promoter, the CpG region predicted to be a consensus FOXA2 binding (FB) site was analyzed.

(B, C, E, and F) Levels of 5hmC/5mC and H3K27m3/H3K9m3 in the promoter regions of *Foxa2* (B and C) and *Lmx1a* (E and F) in undifferentiated (d0) and differentiated (d6) VM-NSC cultures. Data are presented as $\log_2$ values of the fold changes (VC^+/VC^-). N/A, not amplified.

(G and H) TET1, JMJD3, and JMJD2 protein recruitments to the *Foxa2* (G) and *Lmx1a* promoters (H) at d0.

(legend continued on next page)

mDA neurons was critical for survival, phenotype maintenance, and functions of this neuronal type. Of note, the percentage of FOXA2$^+$ and LMX1A$^+$ cells increased by VC treatment during the NSC stage was sustained after differentiation (after VC withdrawal) (Figure 3A, graph); this was directly associated with increased FOXA2/LMX1A expression in differentiated DA neurons (Figures 2B and 2C) and, thus, enhanced DA neuron survival and presynaptic function (Figures 2F–2J).

Next, we sought to determine how VC promoted FOXA2 and LMX1A expression in proliferating VM-NSCs. VC treatment enhanced the mRNA levels of *Foxa2* and *Lmx1a* (Figure 3B), indicating that VC acted at the gene transcription level. In addition to its anti-oxidant role, VC acts as a cofactor for the family of Fe(II)-2-oxoglutarate-dependent dioxygenases (Loenarz and Schofield, 2008), including epigenetic control enzymes such as ten-eleven-translocation 1–3 (TET1–3) and Jumonji C (JmjC)-domain-containing histone demethylases (JMJDs) (He et al., 2015). VC treatment of proliferating VM-NSCs greatly enhanced TET enzyme activity in nuclear fractions (Figure 3C), with which methylated cytosine on CpG sites (5-methylcytosine [5mC]) of DNA is hydroxylated into 5-hydoxymethylcytosine (5hmC). Consequently, global 5hmC levels estimated by immunoblotting (Figure 3D) and immunocytochemical (Figure 3E) analyses were greatly increased in VC-treated VM-NSCs; this was accompanied by a significant decrease in global 5mC levels (Figures 3F and 3G). The increase in JMJD enzyme activity was observed in the nuclear fractions of VC-treated VM-NSCs (Figure 3H). Among the histone methylations tested, global levels of H3K27m3 and H3K9m3 were reduced by VC treatment (Figures 3I–3K).

Based on these findings, we assessed 5hmC/5mC and H3K27m3/H3K9m3 levels in the promoter regions of *Foxa2* and *Lmx1a* (Figures 4A and 4D). Hydroxymethylated DNA immunoprecipitation qPCR (hMeDIP-qPCR) and MeDIP-qPCR analyses revealed that in the *Foxa2* promoter regions 5hmC was more abundant in VC-treated NSCs, while 5mC levels were reduced (Figure 4B). We further observed a decrease in H3K27m3 and H3K9m3 levels in the *Foxa2* promoter regions after VC treatment (Figure 4C). Similar VC-mediated epigenetic changes were also observed in a CpG-abundant region of the *Lmx1a* gene promoter (Figures 4E and 4F). Notably, recruitment of TET1, JMJD3, and JMJD2 proteins to the *Foxa2* and *Lmx1a* promoter regions in VM-NSCs was dramatically increased by VC treatment (Figures 4G and 4H), indicating that the epigenetic enzyme abundance in the promoters, along with their enzyme activity increases, contributed to the observed VC-induced epigenetic changes at the promoter regions. In the developing brain, intracellular VC contents are much higher than in extracellular fluids due to the action of sodium-dependent VC transporter 2 (SVCT2) transporting VC into the intracellular space against its gradient in a sodium- and pH-dependent manner (Tsukaguchi et al., 1999). Blocking SVCT2 action by lowering pH or by treatment with quercetin, a specific SVCT2 inhibitor (Gess et al., 2010; Liang et al., 2001), abolished the VC-mediated changes to 5mC/5hmC and H3K27m3/H3K9m3 on the *Foxa2* and *Lmx1a* genes (Figures 4I and 4J). These findings collectively demonstrated the direct action of VC on observed epigenetic changes. As DNA hydroxymethylation/demethylation and histone demethylation are associated with open DNA/chromatin structures, the VC-induced epigenetic changes in the *Foxa2* and *Lmx1a* promoters were responsible for the observed gene expression increases. In addition, considering the actions of FOXA2 and LMX1A as the master regulators of mDA neuron development, the VC-mediated epigenetic controls in those master genes are proposed to be the central mechanism for the effects of VC on enhanced mDA neuron differentiation. Interestingly, the VC-mediated changes in 5mC/5hmC and H3K27m3/H3K9m3 in *Foxa2* and *Lmx1a* were maintained in the differentiated cells long after VC withdrawal (Figures 4B, 4C, 4E, and 4F). The sustained open DNA/chromatin structures of these genes likely contributed to sustained FOXA2 and LMX1A expression in DA neurons in differentiated cultures, as shown in Figures 2B and 2C.

It has been reported that open epigenetic signatures on late developmental/differentiated phenotype genes are frequently established during an early stage of stem cell differentiation, without their actual expression (Mikkelsen et al., 2007). Thus, we further examined the effect of VC on epigenetic changes in later mDA developmental and differentiated genes. NURR1, the transcription factor critical for DA phenotype gene expression, begins to be expressed from late mDA neuron progenitor cells (Saucedo-Cardenas et al., 1998; Zetterstrom et al., 1996). Consistent with this, NURR1-expressing cells were not detected in proliferating VM-NSC stages (d0), but began to be detected from d2 (Figures 5A and 5B). The percentage of NURR1$^+$ cells at d2 was greater in cultures treated with VC during the proliferating NSC stage, and this increase in NURR1 expression was sustained during the later

(I and J) The VC-induced epigenetic changes on the *Foxa2* (I) and *Lmx1a* (J) promoters was abolished by blocking SVCT activity by lowering pH (pH 5) and with treatment by the SVCT2 inhibitor, quercetin (10 μM). The inhibitors and vehicle (−) were treated for 3 hr prior to VC treatment. The levels of the epigenetic proteins and codes were determined in regions.
Significance at *p < 0.05, **p < 0.01, ***p < 0.001, n = 3 independent experiments, t test.

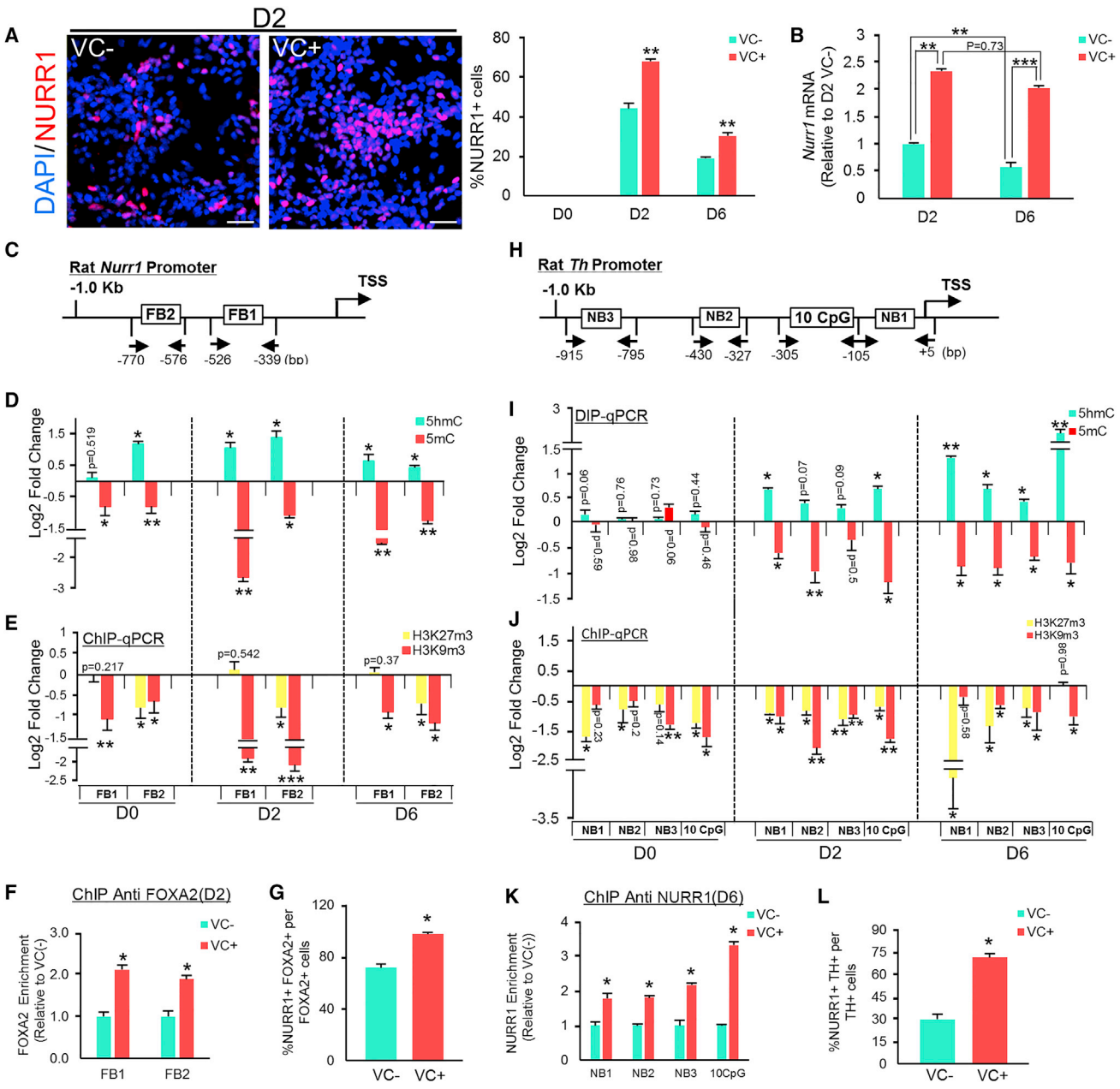

Figure 5. VC-Induced Epigenetic Changes in Later Developmental and Differentiated mDA Neuronal Genes

Undifferentiated VM-NSCs proliferated in the presence (VC$^+$) or absence of VC (VC$^-$), then differentiation without VC for 6 days.

(A and B) Expression of the later mDA developmental gene *Nurr1* assessed by immunocytochemical (A) and real-time qPCR (B) analyses. **p < 0.01, ***p < 0.001, n = 3 independent experiments, Student's t test. Scale bar, 50 μm.

(C–G) Effects of VC pretreatment on the levels of 5hmC/5mC and H3K27m3/H3K9m3 on the *Nurr1* promoter. (C) Schematic for the rat *Nurr1* promoter with consensus FOXA2 binding sites (FB) targeted for the DIP- and ChIP-PCR analyses. The hMeDIP/MeDIP-qPCR for 5hmC/5mC (D) and ChIP-qPCR analyses for H3K27m3/H3K9m3 (E) were carried out over the differentiation period (d0–d6). (F and G) Along with increases of FOXA2 protein recruitment to the *Nurr1* promoter at d2, n = 3 independent experiments (F), the percentage of FOXA2$^+$,NURR1$^+$ cells among total NURR1$^+$ cells, n = 3 independent experiments (G) was greater in cultures differentiated from VC-treated NSCs. *p<0.05; **p<0.01; ***p<0.001, t-test.

(legend continued on next page)

differentiation period (Figures 5A and 5B). Interestingly, compared with untreated controls, increased 5hmC levels with 5mC decreases and the decrease of H3K27m3/H3K9m3 at *Nurr1* promoter regions (consensus FOXA2 binding sites, Figure 5C) were observed in the VC-treated cultures from the undifferentiated stage (d0) (Figures 5D and 5E) when no NURR1 expression was detected (Figure 5A, graph). These epigenetic code changes became greater at d2 and were maintained at least up to d6. Along with the activated epigenetic patterns associated with open DNA/chromatin structures, FOXA2, a transcription factor known to directly induce NURR1 transcription (Yi et al., 2014), was more abundantly recruited to the *Nurr1* promoter regions at d2 in the culture pretreated with VC (Figure 5F). Consequently, the percentage of $FOXA2^+$ cells co-expressing NURR1 at d2 was significantly greater in cultures pretreated with VC (Figure 5G).

VC treatment during the proliferation period also induced similar epigenetic changes (except 5hmC/5mC at d0) on the *Th* promoter (Figure 5H), a DA phenotype gene expressed in terminally differentiated DA neurons, from d0 (Figures 5I and 5J). There was an increasing trend in the activated epigenetic code levels, especially in 5hmC at *Th* promoters, during the 6 days of differentiation. Consistent with this, chromatin immunoprecipitation (ChIP)-qPCR analyses showed significantly greater NURR1 protein abundance at the consensus NURR1 binding sites and a CpG-enriched site (close to the transcription start site) of the *Th* promoter at d6 in VC-pretreated cultures (Figure 5K), resulting in an enhanced ability of NURR1 to induce TH expression (percent $NURR1^+$,TH^+ of total $NURR1^+$ cells) upon VC pretreatment (Figure 5L). Again, the VC-induced epigenetic changes to the *Nurr1* and *Th* gene promoters were abolished by blocking SVCT2 activity (Figure S3). VC administration to proliferating VM-NSCs did not affect the epigenetic codes on the other neuronal subtype genes such as tryptophan hydroxylase 2 (*Tph2*, serotonergic neurons) and glutamic acid decarboxylase 67 (*GAD67*, GABAergic) (Figures S4A and S4B) along with no significant alteration in their mRNA expression levels (Figure S4D). By contrast, VC-mediated changes to 5hmC/5mC and H3K27m3/H3K9m3 levels observed in the *Th* promoter were similarly detected in the promoter of glial fibrillary acidic protein (*Gfap*), specific for astrocytes (consensus STAT binding region) (Figure S4C). Consistently, mRNA expression of *Gfap* as well as $GFAP^+$ astrocyte yields were significantly enhanced by VC pretreatment (Figures S5D and S5E). In summary, we showed that VC treatment of proliferating VM-NSCs induced epigenetic changes into open DNA/chromatin structures in a range of DA neuron developmental genes specific to early (*Foxa2*, *Lmx1a*) and intermediate (*Nurr1*) mDA neuron progenitors and terminally differentiated DA neurons (*Th*). The VC-mediated epigenetic changes in these genes were sustained long after VC withdrawal, including in terminally differentiated mDA neurons. Thus, sustained epigenetic changes resulting from transient VC treatment of proliferating VM-NSCs were responsible for enhanced DA neuron differentiation and sustained midbrain-specific factor expression in differentiated mDA neuronal cells.

Cell Transplantation in PD Rats

Based on the *in vitro* findings, we ultimately assessed the therapeutic functions of VM-NSCs expanded with VC supplementation in a PD animal model. For this experiment, rat E12 VM-NSCs were expanded *in vitro* for 8 days (passaged at day 4 of proliferation) in the presence or absence of VC (P1 d0), harvested, and intrastriatally transplanted into a hemi-parkinsonian rat model. While functional recovery of PD rats has been demonstrated using transplantation of short-term expanded NSCs derived from early embryonic VM tissues (Jensen et al., 2008; Kim et al., 2003; Studer et al., 1998; Timmer et al., 2006), this would not be expected to be achieved by transplanting NSCs expanded and passaged for a longer period due to the loss of DA neurogenic potentials (Jensen et al., 2008; Lee et al., 2003; Timmer et al., 2006; Yan et al., 2001), loss of midbrain-specific factor expression, and poor cell survival during and after differentiation (Anderson et al., 2007; Ko et al., 2009; Rhee et al., 2011). As expected, an amphetamine-induced rotation test revealed no significant reduction in rotation scores compared with pretransplantation values in PD rats grafted with control NSCs (n = 7). In contrast, dramatic behavioral recoveries were achieved in animals grafted with VM-NSCs expanded in the presence of VC. In all eight rats grafted with VC-pretreated NSCs, without exception, rotations were reduced at 8 weeks post transplantation (Figures 6A–6C). In the stepping test (Figure 6D), rats grafted with VC-pretreated NSCs used their lesioned (left) forelimbs more often than did rats grafted with control NSCs. The percentage of adjusting steps of the lesion-containing paw was 37.3% ± 3.9%

(H–J) Effects of VC pretreatment on the levels of 5hmC/5mC and H3K27m3/H3K9m3 in the *Th* gene promoter regions. DIP- and ChIP-PCR analyses were performed to assess epigenetic code changes in consensus NURR1 binding (NB) and 10 CpG sites of the rat *Th* promoter over the differentiation period (d0–d6). $^*p < 0.05$, $^{**}p < 0.01$, n = 3 independent experiments, Student's t test.

(K) NURR1 protein recruitment to the *Th* promoter regions at d6, n = 3 independent experiments. $^*p < 0.05$, Student's t test.

(L) NURR1 efficiency in inducing TH expression estimated by the percentage of $NURR1^+$,TH^+ cells among total $NURR1^+$ cells at d6. $^*p < 0.05$, n = 3 independent experiments, Student's t test.

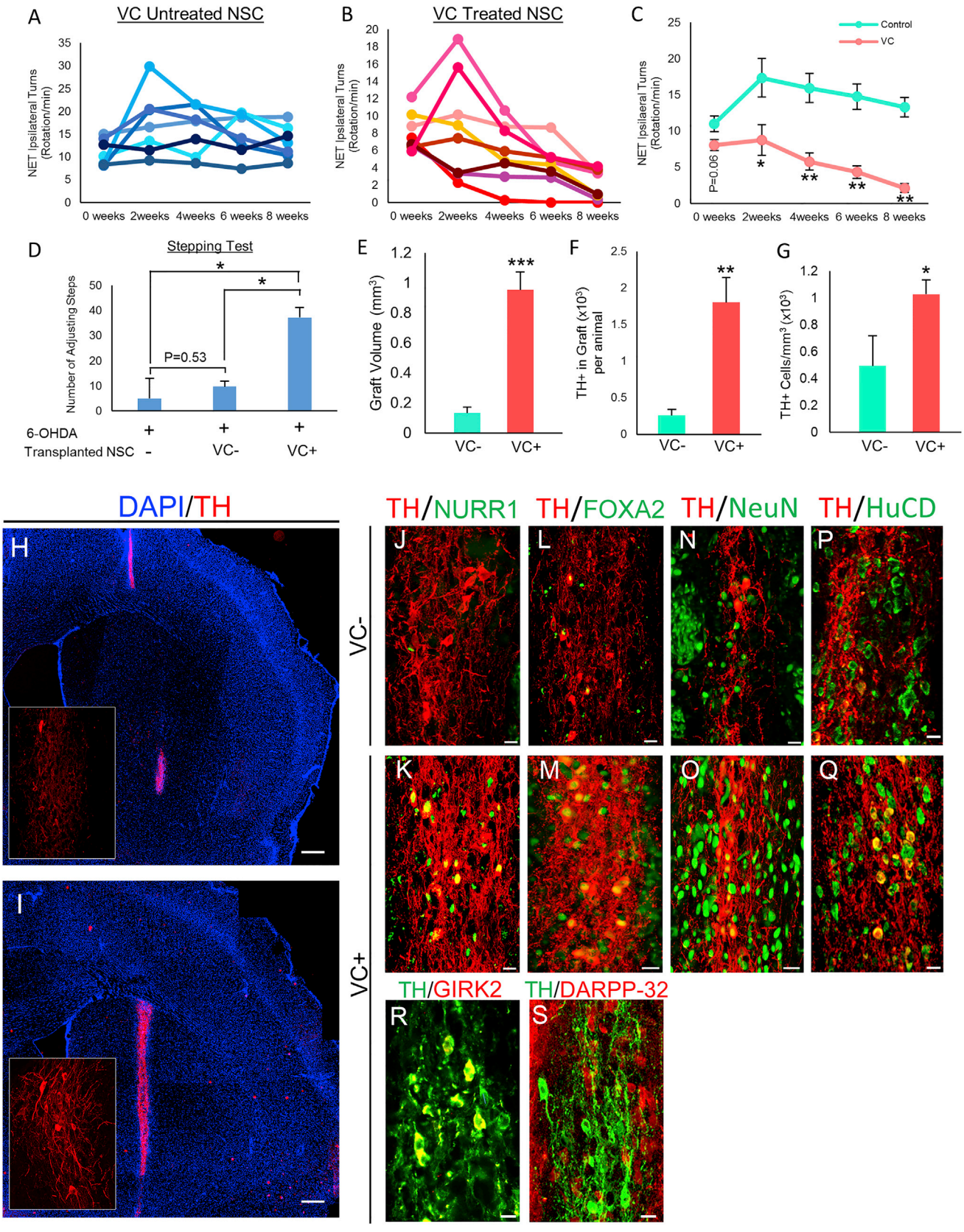

(legend on next page)

(VC) versus 9.7% ± 2.2% (control) of the right unlesioned paw, n = 7 (control) and n = 8 (VC), $p = 7.3 \times 10^{-8}$, ANOVA followed by Tukey's post hoc analysis.

Consistent with the observed increased survival of differentiating/differentiated cells from VC-pretreated NSCs *in vitro* (Figures 2G–2J), histological analyses performed 8 weeks post transplantation exhibited much larger graft formation in rats transplanted with VC-treated NSCs than control NSCs (0.95 ± 0.11 mm^3 in VC group, n = 8 versus 0.13 ± 0.04 in the control group, n = 7, $p = 1.4 \times 10^{-4}$, Student's t test, Figures 6E, 6G, 6H, and 6I). Consistently, more abundant cleaved caspase-3^+ apoptotic cells in grafts were detected in the control group compared with the VC group (Figure S5A). None in the control and VC-treated NSC grafts were positive for the proliferating cell markers of proliferating cell nuclear antigen and phospho-histone H3 (Figures S5B and S5C). There were 1,802 ± 338 TH^+ cells (VC) versus 260 ± 78 TH^+ cells (control) in the graft per animal (Figure 6F). However, the cell densities of general neuronal (HuC/D^+, Figure S5D) and serotonergic neuronal cells (5-hydroxytryptamine; 5-HT^+, Figure S5E) were not significantly different between the control and VC grafts. Consistent with the observed *in vitro* VC effects on astrocytic differentiation (Figures S4D and S4E), $GFAP^+$ astrocytes were greater in the grafts generated by VC-treated NSCs (Figure S5F). TH^+ cells in the VC-treated NSC grafts exhibited more mature neuronal shapes than those in the control grafts (Figures 6H and 6I, insets). In addition, there was a very clear difference in the co-expression of markers specific for mature mDA neurons in TH^+ cells, whereby in the control grafts virtually none or a few of the TH^+ cells were positive for mature neuronal and mDA neuronal markers (Figures 6J, 6L, 6N, and 6P). These findings are consistent with lack of mature neuron formation from grafted NSCs (Park et al., 2006; Yi et al., 2008) and the loss of NURR1 and FOXA2 expression in stressful environments (Oh et al., 2015). In clear contrast, expression of mature neuronal (NeuN and HuC/D) and mDA neuronal (FOXA2, NURR1, and GIRK2) markers was faithfully co-localized in virtually all TH^+ cells in the grafts generated by VC-treated NSC transplantation (Figures 6K, 6M, 6O, 6Q, and 6R). The TH^+ mDA neurons in the graft were neighbored by cells positive for dopamine and cyclic AMP-regulated phosphoprotein 32 (DARPP-32), a marker for striatal postsynaptic neurons receiving signal from nigral mDA neurons (Figure 6S). These findings collectively suggest that VC treatment during VM-NSC expansion yielded therapeutically competent donor cells for use in cell therapeutic approaches to treating PD.

DISCUSSION

The most serious drawback associated with utilizing tissue-specific stem cell cultures in research and therapies is that their original properties and functionalities are altered during *in vitro* culturing. Cultured cells are expected to be exposed to cellular stresses during *in vitro* cell expansion and passaging. Since ROS is a major molecule causing loss of cell functionality associated with injury and aging, we tested whether scavenging ROS by anti-oxidant treatment could rescue the loss of DA neurogenic potential that occurs during culture of VM-NSCs. Our data showed that none of the anti-oxidants tested, except VC, prevented this culture-dependent change. In addition, inhibition of cell senescence by treatment with SB202190 (a P38-MAPK inhibitor) had no rescuing effect (data not shown), suggesting that ROS or cellular aging/senescence was not the mechanism responsible for the loss of DA neuron yield in cultured VM-NSCs. By contrast, cellular aging/senescence is a leading molecular mechanism causing loss of functionality in stem cells present in adult tissues (reviewed in Signer and Morrison, 2013), and anti-senescence reagents could prevent culture-dependent changes in stem cell cultures derived from adult tissues (Cosgrove et al., 2014). As DA neuron formation occurred in VM

Figure 6. VC-Treated NSC Transplantation into Parkinson's Disease Rat Model

NSCs derived from rat embryonic VM at E12 were expanded *in vitro* with or without VC for 8 days. The donor cells were harvested (equivalent to P2 culture), and intrastriatally transplanted into 6-OHDA-lesioned PD model rats. Behavioral (A–D) and histological (E–S) analyses were carried out during or at 8 weeks post transplantation.

(A–D) Amphetamine-induced rotation scores. The ipsilateral net rotation values of individual animals transplanted with control NSCs (A) and VC-NSCs (B) and their mean ± SEM (C) are depicted. n = 8 rats (VC-NSC), n = 7 rats (control NSC). Significant differences from the control at each post-transplantation time point at $^*p < 0.05$ and $^{**}p < 0.01$, two-way ANOVA. Behaviors of the transplanted animals were further assessed by Stepping test (D) at 8 weeks post transplantation: $^*p < 0.001$, ANOVA followed by Tukey's post hoc analysis.

(E–S) Histological analyses 8 weeks post transplantation. (E–G) Graft volume (E), total number of TH^+ cells in graft per animal (F), and TH^+ cell density in graft (G). $^*p < 0.05$, $^{**}p < 0.01$, $^{***}p < 0.001$, t test. (H and I) Overviews of TH^+ cell grafts. Insets show TH^+ DA neuron morphology in grafts shown at high magnification. (J–R) Co-expression of mature neuronal (HuC/D and NeuN) (N–Q), midbrain-specific (FOXA2 and NURR1) (J–M), and A9 nigral mDA neuronal (GIRK2) (R) markers in TH^+ DA cells at 8 weeks post transplantation. (S) DARPP-32^+ striatal neurons adjacent to TH^+ cells in the VC-NSC graft.

Scale bars, 500 μm (H and I) and 30 μm (J–S).

tissues at an early embryonic stage, our cultures were derived from embryonic VMs. Based on these findings, it was likely that cellular aging/senescence was not the critical factor responsible for the functionality changes in cultured stem cells derived from embryonic tissues, although it was the major mechanism for loss of stem cell functions derived from adult tissues. Instead, the culture-dependent changes of the NSCs derived from embryonic tissues were likely to be associated with the developmental program, in which DA neurogenic potential was physiologically lost in late NSCs that underwent several additional rounds of cell cycling in the developing VM as development proceeded.

The expression of midbrain factors FOXA2 and NURR1 is critical for mDA neuron survival, function, and phenotype maintenance (Decressac et al., 2013; Oh et al., 2015). However, expression of these factors disappears in aged and toxic environments (Oh et al., 2015). Similarly, grafted mDA neurons easily undergo loss of midbrain factor expression in hostile brain environments (Figure 6 and Rhee et al., 2016). Therefore, expression of midbrain-specific factors in grafted mDA neurons is critical for the success of cell therapy for PD (Kriks et al., 2011). In addition to increased DA neuronal yield, VC pretreatment of donor NSCs maintained midbrain marker expression in grafted mDA neurons long after transplantation, which was closely related to enhanced grafted cell survival and functions, and ultimately enhanced therapeutic outcomes. Another characteristic of NSCs altered during *in vitro* expansion as well as *in vivo* brain development is transition of NSC differentiation propensity from neuronal to astrocytic differentiation (Figures S4D and S4E; Anderson et al., 2007; Chang et al., 2004a, 2004b; Qian et al., 2000). Based on the observed effect of VC in preventing culture-dependent changes, it was expected that VC could also prevent neuron-to-astrocyte transition during *in vitro* culturing. However, contrary to our expectations, VC treatment rather strongly enhanced astrocytic differentiation from cultured VM-NSCs via DNA/histone demethylation in the *Gfap* promoter region (Figure S4C), indicating that VC-mediated effects on VM-NSC cultures are not completely associated with prevention of culture- or development-dependent processes. Based on the physiologic neurotrophic actions of brain astrocytes (Horner and Palmer, 2003; Nedergaard et al., 2003), transplantation of astrocytes alone or together with neurogenic donor cells has become a therapeutic possibility for treating intractable brain disorders (Chen et al., 2015). Thus, the VC effect on astrocyte differentiation is another beneficial contributor to attain improved therapeutic outcomes achieved by transplanting VC-treated NSCs, whereby astrocytes differentiated from the grafted NSCs exert trophic support for neuronal differentiation/maturation and survival in grafted brains. It was noted that TH^+ DA neuronal cells in the grafts formed by VC-treated NSCs were more abundantly surrounded by $GFAP^+$ astrocytes (Figure S5F).

In this study, we demonstrated that VC exerted its observed effects via DNA/histone demethylation-based epigenetic control on DA neuron developmental genes. A similar epigenetic control mechanism was demonstrated in our previous study by treatment with VC during NSC differentiation (He et al., 2015). However, epigenetic regulation and gene expression induced by VC treatment of differentiating NSCs was limited to terminally differentiated DA neuron genes such as *Th* and *Dat*. Thus, without effects on the expression of midbrain-specific factors and differentiated cell survival, the therapeutic value of the previous VC treatment method seems to be marginal. By contrast, the effect of VC treatment during NSC expansion covered changes in a wide range of mDA neuron developmental and phenotype genes, such as those acting at early undifferentiated stages of VM-NSCs (*Foxa2*, *Lmx1a*), intermediate mDA neuron progenitors (*Nurr1*), and terminally differentiated mDA neurons (*Th*). Interestingly, the epigenetic status of those genes was maintained in differentiated mDA neurons long after VC withdrawal. These findings suggest that transient VC treatment can induce a stable and long-lasting epigenetic change in mDA neuronal genes. It is also possible that VC treatment only triggers the mDA neuron developmental cascade by directly promoting the expression of FOXA2 and LMX1A, the master regulators expressed in undifferentiated VM-NSCs. Induction of the later developmental factor expressions subsequently follows in the facilitated developmental cascade. The later developmental factors may take over VC-mediated epigenetic regulatory actions and contribute to the maintenance of the epigenetic status during later differentiation stages. Consistent with this, the epigenetic opening roles of FOXA2, NURR1, and PITX3 on DA phenotype genes have previously been reported (Jacobs et al., 2009; Yi et al., 2014). Regardless of the mechanism, the sustained open DNA/chromatin structures surely contributed to the generation of mDA neurons expressing midbrain-specific markers and promoted resistance to toxic stimuli both *in vitro* and *in vivo* long after transplantation.

For the application of VC treatment in the clinical setting of PD cell therapy, the VC effects observed in this study should be replicated in human NSC cultures. Thus, we treated proliferating NSCs derived from human embryonic stem cells (hESCs) (Rhee et al., 2011) with VC, and differentiation of the human NSCs was induced without VC. Similar to rodent VM-NSC cultures, VC pretreatment greatly promoted differentiating/differentiated cell survival in hESC-NSC cultures (Figure S6A). In addition, TH^+ DA neuronal yields were significantly enhanced in the

cultures differentiated from the VC-pretreated human NSCs (Figure S6B). Compared with untreated control cultures, TH^+ cells in the VC-pretreated cultures exhibited more extensive neurite branching (Figure S6C). Along with an increase in *TH* mRNA expression (Figure S6D), the levels of 5hmC at human *TH* promoter regions (two consensus NURR1 binding sites; NGFI-B response element) were enhanced at the expense of 5mC levels by VC pretreatment, but H3K9m3/H3K27m3 levels, which significantly decreased in the rat *Th* promoter after VC pretreatment, were undetectable in the human *TH* promoter regions (Figure S6E), indicating similarity and dissimilarity between rodent and human *TH* promoters in VC-mediated epigenetic control. We could not assess VC effects on midbrain-specific gene expressions in human NSCs, since the hESC-derived NSCs partially adopt VM phenotypes (Kriks et al., 2011), and authentic human VM-NSC cultures are currently not available. Although further assessments are required in authentic human VM-NSC cultures when they are available, the observed benefits of VC pretreatment in human NSC-DA differentiation and differentiated cell survival are at least applicable in PD cell therapeutic approaches. Given the high VC levels in brain cells (Harrison and May, 2009), VC treatment is physiologic. VC treatment of donor cells was simple and safe without necessity for VC supplementation into the grafted brain. Therefore, use of this VC pretreatment strategy during preparation of donor NSCs could become a PD cell therapy option in the clinical setting.

EXPERIMENTAL PROCEDURES

Cell Culture

NSCs were cultured from rat embryo VMs (Sprague-Dawley) at E12 or derived by *in vitro* differentiation of hESCs (H9) as previously described (Rhee et al., 2011). The methods are described in detail in Supplemental Experimental Procedures.

Epigenetic Assays

Determination of TET and JMJD enzyme activities, global 5mC/5hmC and H3K9m3/H3K27m3 levels, ChIP-qPCR and DIP-qPCR analyses were carried out as previously described (He et al., 2015) and are described in detail in Supplemental Experimental Procedures.

In Vivo Animal Experiments

All procedures for animal experiments were approved by the Institutional Animal Care and Use Committee at Hanyang College of Medicine (approval number 2014-0212A). Experiments were performed in accordance with NIH guidelines. Hemi-parkinsonism was induced in adult female Sprague-Dawley rats (220–250 g) by unilateral stereotactic injection of 3 μL of 6-OHDA (8 μg/μL; Sigma). Transplantation and histological procedures are described in Supplemental Experimental Procedures.

Cell Counting and Statistical Analysis

Immunostained cells were counted in 10–20 random areas of each culture coverslip using an eyepiece grid at a magnification of 200×. All data are expressed as the mean ± SEM of three to eight independent experiments. Statistical comparisons were made using Student's t test (unpaired) or one-way ANOVA followed by Tukey's post hoc analysis using SPSS Statistics 21 (IBM). The relevant n and p values, and statistical analysis methods are indicated in each figure legend.

SUPPLEMENTAL INFORMATION

Supplemental Information includes Supplemental Experimental Procedures, six figures, and three tables and can be found with this article online at http://dx.doi.org/10.1016/j.stemcr.2017.08.017.

AUTHOR CONTRIBUTIONS

N.W., conception and design, collection and/or data assembly, data analysis and interpretation, manuscript writing, and final approval of manuscript; E.-H.K., collection and/or data assembly, data analysis and interpretation, and manuscript writing; J.-J.S., Y.-H.R., and Y.A.S., collection and/or data assembly; S.-H.L., conception and design, financial support, administrative support, provision of study material, data analysis and interpretation, manuscript writing, and final approval of manuscript.

ACKNOWLEDGMENTS

This work was supported by grants from the Medical Research Center (2017R1A5A2015395) and NRF-2017R1A2B2002220, funded by the National Research Foundation of Korea (NRF) of the Ministry of Science and ICT, Republic of Korea.

Received: December 20, 2016
Revised: August 24, 2017
Accepted: August 24, 2017
Published: September 21, 2017

REFERENCES

Anderson, L., Burnstein, R.M., He, X., Luce, R., Furlong, R., Foltynie, T., Sykacek, P., Menon, D.K., and Caldwell, M.A. (2007). Gene expression changes in long term expanded human neural progenitor cells passaged by chopping lead to loss of neurogenic potential in vivo. Exp. Neurol. *204*, 512–524.

Chang, M.Y., Park, C.H., Lee, S.Y., and Lee, S.H. (2004a). Properties of cortical precursor cells cultured long term are similar to those of precursors at later developmental stages. Brain Res. Dev. Brain Res. *153*, 89–96.

Chang, M.Y., Park, C.H., Son, H., Lee, Y.S., and Lee, S.H. (2004b). Developmental stage-dependent self-regulation of embryonic cortical precursor cell survival and differentiation by leukemia inhibitory factor. Cell Death Differ. *11*, 985–996.

Chen, C., Chan, A., Wen, H., Chung, S.H., Deng, W., and Jiang, P. (2015). Stem and progenitor cell-derived astroglia therapies for neurological diseases. Trends Mol. Med. *21*, 715–729.

Chung, S., Leung, A., Han, B.S., Chang, M.Y., Moon, J.I., Kim, C.H., Hong, S., Pruszak, J., Isacson, O., and Kim, K.S. (2009). Wnt1-lmx1a forms a novel autoregulatory loop and controls midbrain dopaminergic differentiation synergistically with the SHH-FoxA2 pathway. Cell Stem Cell *5*, 646–658.

Cosgrove, B.D., Gilbert, P.M., Porpiglia, E., Mourkioti, F., Lee, S.P., Corbel, S.Y., Llewellyn, M.E., Delp, S.L., and Blau, H.M. (2014). Rejuvenation of the muscle stem cell population restores strength to injured aged muscles. Nat. Med. *20*, 255–264.

Decressac, M., Volakakis, N., Bjorklund, A., and Perlmann, T. (2013). NURR1 in Parkinson disease—from pathogenesis to therapeutic potential. Nat. Rev. Neurol. *9*, 629–636.

Dunnett, S.B., Bjorklund, A., and Lindvall, O. (2001). Cell therapy in Parkinson's disease—stop or go? Nat. Rev. Neurosci. *2*, 365–369.

Freed, C.R., Greene, P.E., Breeze, R.E., Tsai, W.Y., DuMouchel, W., Kao, R., Dillon, S., Winfield, H., Culver, S., Trojanowski, J.Q., et al. (2001). Transplantation of embryonic dopamine neurons for severe Parkinson's disease. N. Engl. J. Med. *344*, 710–719.

Gess, B., Lohmann, C., Halfter, H., and Young, P. (2010). Sodium-dependent vitamin C transporter 2 (SVCT2) is necessary for the uptake of L-ascorbic acid into Schwann cells. Glia *58*, 287–299.

Harrison, F.E., and May, J.M. (2009). Vitamin C function in the brain: vital role of the ascorbate transporter SVCT2. Free Radic. Biol. Med. *46*, 719–730.

He, X.B., Kim, M., Kim, S.Y., Yi, S.H., Rhee, Y.H., Kim, T., Lee, E.H., Park, C.H., Dixit, S., Harrison, F.E., et al. (2015). Vitamin C facilitates dopamine neuron differentiation in fetal midbrain through TET1- and JMJD3-dependent epigenetic control manner. Stem Cells *33*, 1320–1332.

Hof, P.R., and Morrison, J.H. (2004). The aging brain: morphomolecular senescence of cortical circuits. Trends Neurosci. *27*, 607–613.

Horner, P.J., and Palmer, T.D. (2003). New roles for astrocytes: the nightlife of an 'astrocyte'. La vida loca!. Trends Neurosci. *26*, 597–603.

Jacobs, F.M., van Erp, S., van der Linden, A.J., von Oerthel, L., Burbach, J.P., and Smidt, M.P. (2009). Pitx3 potentiates Nurr1 in dopamine neuron terminal differentiation through release of SMRT-mediated repression. Development *136*, 531–540.

Jensen, P., Pedersen, E.G., Zimmer, J., Widmer, H.R., and Meyer, M. (2008). Functional effect of FGF2- and FGF8-expanded ventral mesencephalic precursor cells in a rat model of Parkinson's disease. Brain Res. *1218*, 13–20.

Kim, J.Y., Koh, H.C., Lee, J.Y., Chang, M.Y., Kim, Y.C., Chung, H.Y., Son, H., Lee, Y.S., Studer, L., McKay, R., et al. (2003). Dopaminergic neuronal differentiation from rat embryonic neural precursors by Nurr1 overexpression. J. Neurochem. *85*, 1443–1454.

Kim, M., Kim, C., Choi, Y.S., Kim, M., Park, C., and Suh, Y. (2012). Age-related alterations in mesenchymal stem cells related to shift in differentiation from osteogenic to adipogenic potential: implication to age-associated bone diseases and defects. Mech. Ageing Dev. *133*, 215–225.

Ko, J.Y., Lee, H.S., Park, C.H., Koh, H.C., Lee, Y.S., and Lee, S.H. (2009). Conditions for tumor-free and dopamine neuron-enriched grafts after transplanting human ES cell-derived neural precursor cells. Mol. Ther. *17*, 1761–1770.

Kratzing, C.C., Kelly, J.D., and Kratzing, J.E. (1985). Ascorbic acid in fetal rat brain. J. Neurochem. *44*, 1623–1624.

Kriks, S., Shim, J.W., Piao, J., Ganat, Y.M., Wakeman, D.R., Xie, Z., Carrillo-Reid, L., Auyeung, G., Antonacci, C., Buch, A., et al. (2011). Dopamine neurons derived from human ES cells efficiently engraft in animal models of Parkinson's disease. Nature *480*, 547–551.

Lee, J.Y., Koh, H.C., Chang, M.Y., Park, C.H., Lee, Y.S., and Lee, S.H. (2003). Erythropoietin and bone morphogenetic protein 7 mediate ascorbate-induced dopaminergic differentiation from embryonic mesencephalic precursors. Neuroreport *14*, 1401–1404.

Liang, W.J., Johnson, D., and Jarvis, S.M. (2001). Vitamin C transport systems of mammalian cells. Mol. Membr. Biol. *18*, 87–95.

Loenarz, C., and Schofield, C.J. (2008). Expanding chemical biology of 2-oxoglutarate oxygenases. Nat. Chem. Biol. *4*, 152–156.

Mikkelsen, T.S., Ku, M., Jaffe, D.B., Issac, B., Lieberman, E., Giannoukos, G., Alvarez, P., Brockman, W., Kim, T.K., Koche, R.P., et al. (2007). Genome-wide maps of chromatin state in pluripotent and lineage-committed cells. Nature *448*, 553–560.

Monfort, A., and Wutz, A. (2013). Breathing-in epigenetic change with vitamin C. EMBO Rep. *14*, 337–346.

Nakatani, T., Kumai, M., Mizuhara, E., Minaki, Y., and Ono, Y. (2010). Lmx1a and Lmx1b cooperate with Foxa2 to coordinate the specification of dopaminergic neurons and control of floor plate cell differentiation in the developing mesencephalon. Dev. Biol. *339*, 101–113.

Nedergaard, M., Ransom, B., and Goldman, S.A. (2003). New roles for astrocytes: redefining the functional architecture of the brain. Trends Neurosci. *26*, 523–530.

Oh, S.M., Chang, M.Y., Song, J.J., Rhee, Y.H., Joe, E.H., Lee, H.S., Yi, S.H., and Lee, S.H. (2015). Combined Nurr1 and Foxa2 roles in the therapy of Parkinson's disease. EMBO Mol. Med. *7*, 510–525.

Park, K.I., Hack, M.A., Ourednik, J., Yandava, B., Flax, J.D., Stieg, P.E., Gullans, S., Jensen, F.E., Sidman, R.L., Ourednik, V., et al. (2006). Acute injury directs the migration, proliferation, and differentiation of solid organ stem cells: evidence from the effect of hypoxia-ischemia in the CNS on clonal "reporter" neural stem cells. Exp. Neurol. *199*, 156–178.

Piccini, P., Brooks, D.J., Bjorklund, A., Gunn, R.N., Grasby, P.M., Rimoldi, O., Brundin, P., Hagell, P., Rehncrona, S., Widner, H., et al. (1999). Dopamine release from nigral transplants visualized in vivo in a Parkinson's patient. Nat. Neurosci. *2*, 1137–1140.

Qian, X., Shen, Q., Goderie, S.K., He, W., Capela, A., Davis, A.A., and Temple, S. (2000). Timing of CNS cell generation: a programmed sequence of neuron and glial cell production from isolated murine cortical stem cells. Neuron *28*, 69–80.

Rhee, Y.H., Kim, T.H., Jo, A.Y., Chang, M.Y., Park, C.H., Kim, S.M., Song, J.J., Oh, S.M., Yi, S.H., Kim, H.H., et al. (2016). LIN28A enhances the therapeutic potential of cultured neural stem cells in a Parkinson's disease model. Brain *139*, 2722–2739.

Rhee, Y.H., Ko, J.Y., Chang, M.Y., Yi, S.H., Kim, D., Kim, C.H., Shim, J.W., Jo, A.Y., Kim, B.W., Lee, H., et al. (2011). Protein-based human iPS cells efficiently generate functional dopamine neurons and can

treat a rat model of Parkinson disease. J. Clin. Invest. *121*, 2326–2335.

Saucedo-Cardenas, O., Quintana-Hau, J.D., Le, W.D., Smidt, M.P., Cox, J.J., De Mayo, F., Burbach, J.P., and Conneely, O.M. (1998). Nurr1 is essential for the induction of the dopaminergic phenotype and the survival of ventral mesencephalic late dopaminergic precursor neurons. Proc. Natl. Acad. Sci. USA *95*, 4013–4018.

Savitt, J.M., Dawson, V.L., and Dawson, T.M. (2006). Diagnosis and treatment of Parkinson disease: molecules to medicine. J. Clin. Invest. *116*, 1744–1754.

Signer, R.A., and Morrison, S.J. (2013). Mechanisms that regulate stem cell aging and life span. Cell Stem Cell *12*, 152–165.

Studer, L., Tabar, V., and McKay, R.D. (1998). Transplantation of expanded mesencephalic precursors leads to recovery in parkinsonian rats. Nat. Neurosci. *1*, 290–295.

Timmer, M., Grosskreutz, J., Schlesinger, F., Krampfl, K., Wesemann, M., Just, L., Bufler, J., and Grothe, C. (2006). Dopaminergic properties and function after grafting of attached neural precursor cultures. Neurobiol. Dis. *21*, 587–606.

Tsukaguchi, H., Tokui, T., Mackenzie, B., Berger, U.V., Chen, X.Z., Wang, Y., Brubaker, R.F., and Hediger, M.A. (1999). A family of mammalian Na^+-dependent L-ascorbic acid transporters. Nature *399*, 70–75.

Yan, J., Studer, L., and McKay, R.D. (2001). Ascorbic acid increases the yield of dopaminergic neurons derived from basic fibroblast growth factor expanded mesencephalic precursors. J. Neurochem. *76*, 307–311.

Yi, S.H., He, X.B., Rhee, Y.H., Park, C.H., Takizawa, T., Nakashima, K., and Lee, S.H. (2014). Foxa2 acts as a co-activator potentiating expression of the Nurr1-induced DA phenotype via epigenetic regulation. Development *141*, 761–772.

Yi, S.H., Jo, A.Y., Park, C.H., Koh, H.C., Park, R.H., Suh-Kim, H., Shin, I., Lee, Y.S., Kim, J., and Lee, S.H. (2008). Mash1 and neurogenin 2 enhance survival and differentiation of neural precursor cells after transplantation to rat brains via distinct modes of action. Mol. Ther. *16*, 1873–1882.

Zetterstrom, R.H., Williams, R., Perlmann, T., and Olson, L. (1996). Cellular expression of the immediate early transcription factors Nurr1 and NGFI-B suggests a gene regulatory role in several brain regions including the nigrostriatal dopamine system. Brain Res. Mol. Brain Res. *41*, 111–120.